

Whole-body impedance—what does it measure?^{1,2}

Kenneth R Foster and Henry C Lukaski

ABSTRACT Although the bioelectrical impedance technique is widely used in human nutrition and clinical research, an integrated summary of the biophysical and bioelectrical bases of this approach is lacking. We summarize the pertinent electrical phenomena relevant to the application of the impedance technique in vivo and discuss the relations between electrical measurements and biological conductor volumes. Key terms in the derivation of bioelectrical impedance analysis are described and the relation between the electrical properties of tissues and tissue structure is discussed. The relation between the impedance of an object and its geometry, scale, and intrinsic electrical properties is also discussed. Correlations between whole-body impedance measurements and various bioconductor volumes, such as total body water and fat-free mass, are experimentally well established; however, the reason for the success of the impedance technique is much less clear. The bioengineering basis for the technique is critically presented and considerations are proposed that might help to clarify the method and potentially improve its sensitivity. *Am J Clin Nutr* 1996;64(suppl):388S-96S.

KEY WORDS Resistance, reactance, body composition, fat-free mass, extracellular fluid, total body water

INTRODUCTION

Many papers in the scientific literature report the use of electrical measurements on the human body to estimate total body water, fat-free mass, and other indexes of body composition. Bioelectrical impedance measurements are easy to perform (relative to other measurements of body composition) and instruments are commercially available for the purpose. For these reasons, bioelectrical impedance analysis (BIA) is gaining acceptance outside the clinic and research laboratory.

Many researchers and clinicians, however, have a poor understanding of the bioelectrical principles that underlie the impedance technique. In part, this may reflect a simple unfamiliarity with the biophysical and bioengineering concepts related to the technology. However, the theoretical basis of the technique is also unclear and the literature often presents simple theories relating body impedance measurement to body composition that can be questioned on obvious technical grounds. Indeed, there is no fully satisfactory theory that adequately accounts for the success of the technique.

We review the basic electrical and biophysical principles related to the impedance method. We define impedance and discuss its relation to body impedance measurements. We also summarize the electrical properties of different body tissues.

Finally, we review the theoretical questions regarding the use of bioelectrical impedance measurements made at the distal limbs to predict body-composition variables and suggest potential approaches that might help to clarify the bioelectrical impedance method and improve its accuracy.

BASIC CONCEPTS

The electrical impedance of the body is measured by introducing a small alternating electrical current into the body and measuring the potential difference that results. The impedance magnitude Z is the ratio of the magnitude of the potential difference to the magnitude of the current. With suitable equipment one can also measure the phase difference θ between the voltage and current.

Alternating electrical current flows through the body by several different physical mechanisms. Current flows through physiologic fluids by the movement of ions. This movement is opposed by viscosity and other effects, which can be modeled electrically as a resistance. In addition, the applied current will charge cell membranes and other interfaces, which can be modeled electrically as capacitors. Thus, the impedance of the human body (and of material in general) can be modeled by a combination of capacitive and resistive elements.

A capacitance and a resistance can be combined in two ways: in series or in parallel (**Figure 1**). In either case, the components can be chosen to produce the same impedance of the circuit; however, the component values will differ.

Series-equivalent model

The series-equivalent model shown in Figure 1A consists of a resistor R_s (expressed in Ω) in series with a capacitor C_s (expressed in F). The magnitude of the impedance of this circuit can be written

$$Z = \sqrt{R_s^2 + \frac{1}{(2\pi f C_s)^2}} \quad (1)$$

and the phase difference θ between voltage and current as

$$\theta = -\arctan\left(\frac{1}{2\pi f R C_s}\right) \quad (2)$$

¹ From the Department of Bioengineering, University of Pennsylvania, Philadelphia, and the US Department of Agriculture, Agricultural Research Station, Grand Forks Human Nutrition Research Center, Grand Forks, ND.

² Address reprint requests to KR Foster, Department of Bioengineering, Suite 120 Hayden Hall, 3320 Smith Walk, University of Pennsylvania, Philadelphia, PA 19104-6392. E-mail: kfoster@eniach.seas.upenn.edu.

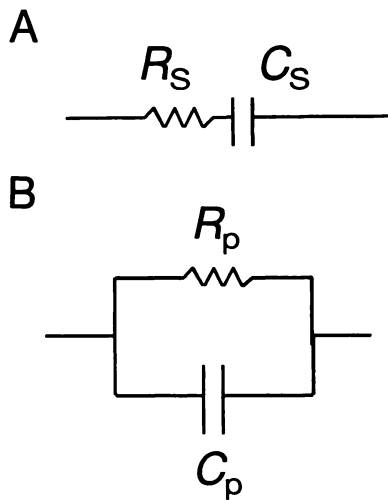


FIGURE 1. Series (A) and parallel (B) combinations of a resistor and capacitor. R_s , series-equivalent resistance, in Ω ; C_s , series-equivalent capacitance, in F; R_p , parallel-equivalent resistance, in Ω ; C_p , parallel-equivalent capacitance, in F.

where f is the frequency (expressed in Hz).

It is often useful to express the impedance of this circuit in terms of a quantity Z^* , which is complex in the mathematical sense:

$$Z^* = R_s - \frac{j}{2\pi f C_s} = R_s + jX \quad (3)$$

where j is the square root of -1 and the asterisk denotes a complex quantity. In the following expression, the quantity X is the reactance of the capacitor, expressed in Ω :

$$X = \frac{-1}{2\pi f C_s} \quad (4)$$

The use of a complex number Z^* to express the impedance is a mathematical device. It allows the investigator to express both measured quantities (the magnitude of the impedance and the phase difference between the voltage and current) in terms of a single quantity, Z^* . Following the usual rules for handling complex quantities, the impedance magnitude Z is the magnitude of the complex quantity Z^* , and the phase angle θ is the arc tangent of the ratio of the imaginary to real parts of Z^* .

Parallel-equivalent model

For reasons discussed below, it is often more convenient to consider instead a parallel circuit consisting of a resistor R_p positioned in parallel with a capacitor C_p (Figure 1B).

The series-equivalent impedance of this circuit can be derived simply by using the rules for addition of parallel circuit elements. In terms of the parallel-equivalent resis-

tance R_p and capacitance C_p , the series-equivalent resistance R_s and reactance X of the circuit can be obtained:

$$R_s = \frac{R_p}{1 + (2\pi f C_p R_p)^2} \quad (5)$$

$$X = \frac{-2\pi f C_p R_p^2}{1 + (2\pi f C_p R_p)^2}$$

The impedance magnitude Z of this circuit is

$$Z = \left[\frac{1}{1/R_p^2 + (2\pi f C_s)^2} \right]^{1/2} \quad (6)$$

and the phase angle θ between voltage and current is

$$\theta = -\arctan(2\pi f C_p R_p). \quad (7)$$

Whether one chooses to interpret impedance measurements in terms of parallel-equivalent elements (R_p and C_p) or series-equivalent elements (R_s and C_s) is a matter of convenience. Most investigators report body impedance data in terms of resistance and reactance, which implicitly refer to a series model as shown in Figure 1A. By contrast, biophysical models of the electrical properties of tissue are more naturally expressed with reference to a parallel model, as shown in Figure 1B.

Intensive and extensive electrical properties

The impedance (or resistance and capacitance) of the human body is an extensive quantity, which like weight or volume depends on body size. It is also useful to consider the intrinsic electrical properties of body tissues, expressed as intensive quantities that (as with temperature) do not depend on body size. Two intensive electrical properties of matter are conductivity (σ) and permittivity (ϵ'). Conductivity is a measure of the amount of current that will flow when an electric field is impressed across the material; permittivity is a measure of the amount of charge that will be induced at interfaces such as cell membranes by the field. Conductivity and permittivity are defined in terms of a parallel-equivalent model because the two electrical processes (conduction of current and accumulation of charge at interfaces) occur independently, ie, in parallel. Resistivity (ρ), which is expressed as $\Omega \cdot \text{m}$, is the inverse of conductivity and is also defined with respect to a parallel-circuit model. Most discussions of the electrical properties of tissue in the biophysical literature are in terms of conductivity; we currently use resistivity because of its more common use in the whole-body impedance literature.

The relation between the extensive properties of a circuit (resistance and capacitance) and the intensive properties of a material (resistivity and permittivity) can be illustrated by considering a simple experiment in which a tissue sample is placed between two electrodes of area A and separation L (Figure 2). The parallel-equivalent resistance (R_p) and capacitance (C_p) of this circuit are related to the resistivity ρ ($\Omega \cdot \text{m}$) and relative permittivity (unitless) of the tissue by the following:

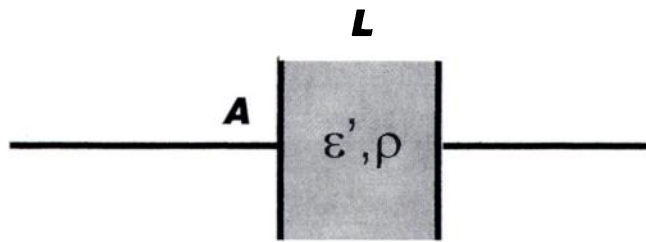


FIGURE 2. Parallel plate capacitor filled with material of known resistivity ρ ($\Omega \cdot m$) and relative permittivity ϵ' . The area of the plates is A and their separation is L .

$$C_p = \epsilon' \epsilon_0 \frac{A}{L} \quad (8)$$

$$R_p = \rho \frac{L}{A}$$

where ϵ_0 is a constant (the permittivity of free space, 8.85 pF/m). The resistance and reactance of the circuit shown in Figure 2 are found by substituting equation 8 into equation 5. The results are as follows:

$$R_s = \frac{L}{A} \left[\frac{\rho}{1 + (2\pi f \epsilon' \epsilon_0 \rho)^2} \right] \approx \frac{L}{A} \rho \quad (9)$$

and

$$X = \frac{-L}{A} \left[\frac{2\pi f \epsilon' \epsilon_0 \rho^2}{1 + (2\pi f \epsilon' \epsilon_0 \rho)^2} \right] \approx \frac{-L}{A} [2\pi f \epsilon' \epsilon_0 \rho^2] \quad (10)$$

where the approximations are valid because $2\pi f \epsilon' \epsilon_0 \rho$ is much less than one for nearly all tissues over the frequency range relevant to BIA. In practical terms, this means that the impedance of the body, at frequencies relevant to BIA, is almost entirely resistive. The reactive (capacitive) contribution is small by comparison.

Both the resistance and reactance of the circuit shown in Figure 2 (or of the body) vary with frequency. This occurs because of the factor f in equation 10 and because the permittivity and resistivity (ϵ' and ρ) are themselves frequency dependent. The permittivity and resistivity of tissues can be

measured experimentally by using a parallel plate arrangement of electrodes similar to that shown in Figure 2. Such measurements yield the electrical properties of the material (σ or ρ and ϵ') that are averaged over distances comparable with the dimensions of the sample (centimeters), which we refer to as bulk properties.

The use of bulk electrical properties of tissue is useful in BIA, which is concerned with the electrical properties of the body on distance scales of centimeters to meters. Thus, it is useful to ignore complexities due to cellular structure and to consider only the bulk electrical properties of tissue. However, the bulk properties can be anisotropic. In particular, the resistivity of muscle varies greatly with direction with respect to the orientation of the muscle fibers. This has important implications for the interpretation of BIA data, which we discuss in a later section.

The preceding discussion shows that the impedance of an object depends on three different factors: its geometry, its scale (eg, physical size), and its intrinsic electrical properties. For the example shown in Figure 2, the scale enters through the factor L/A , and the electrical properties of the material through the resistivity and permittivity. The geometry of the object is implicit in equation 8: the impedance of objects with different geometries would be characterized by different equations entirely.

ELECTRICAL PROPERTIES OF TISSUES AND CELL SUSPENSIONS

The electrical properties of tissues have been studied for many years and a good understanding exists of the relation between the bulk electrical properties of a tissue and its structure; an extensive review is presented elsewhere (1). The elements of tissue structure that are most important include cell size and volume fraction, membrane capacitance, and the conductivity of the intracellular and extracellular media.

The resistivity and permittivity of several tissues at two frequencies (10 kHz and 1 MHz) used in whole-body impedance studies are summarized in **Table 1**. The table also shows the quantities ρ and $2\pi f \epsilon' \epsilon_0 \rho^2$, which are proportional to the real (resistive) and imaginary (reactive) parts of the impedance (equations 9 and 10).

TABLE 1
Permittivity and conductivity of tissues at 37°C¹

Tissue	10 kHz			1 MHz		
	Permittivity (ϵ')	Resistivity (ρ)	Series-equivalent reactance ² ($2\pi f \epsilon' \epsilon_0 \rho^2$)	Permittivity (ϵ')	Resistivity (ρ)	Series-equivalent reactance ² ($2\pi f \epsilon' \epsilon_0 \rho^2$)
Bone	640	$\Omega \cdot m$	$\Omega \cdot m$	87	$\Omega \cdot m$	$\Omega \cdot m$
Fat	30000	15–50	0.03–0.4	NA	15–50	(0.1–1) ³
Blood	2800	1.5	3×10^{-5}	2000	1.5	0.002
Muscle (perpendicular to fibers)	70000	10	0.05	(1900–2500) ⁴	1.3–1.7 ⁴	0.003
Muscle (parallel to fibers)	80000	2	0.001	(1900–2500) ⁴	0.6–0.8 ⁴	0.003

¹ Adapted from reference 1. NA, not applicable.

² Proportional to the series-equivalent reactance; see equation 10.

³ No data available for the permittivity of fat at this frequency; we assume a permittivity of 1000, which is typical of that of other tissues at 1 MHz.

⁴ No data exist for oriented muscle in this frequency range; data are for unoriented muscle. However, anisotropy is less pronounced at high frequencies.

In the tissue-impedance literature there is considerable variability in the reported data, with 2-fold variations in resistivity and 10-fold variations in permittivity often present in data from the same tissue from the same species. In part this might reflect normal biological variability, such as variability in tissue structure and (particularly for adipose tissue) lipid content. Another potential source of variability is the change in tissue properties after death. Many data in the literature were obtained from excised tissues that were far removed from *in vivo* conditions. Twofold increases in resistivity were reported in tissues within a few minutes after blood flow ceased, apparently because of swelling of cells as the result of ischemia (2). In short, some of the variability in the reported data might be important in BIA analysis and other variability might simply reflect experimental artifacts.

The findings listed in Table 1 lead to several important conclusions. At frequencies used in whole-body impedance studies (which are typically in the range of 10 kHz to 1 MHz), tissues are primarily resistive; their reactive components are comparatively small. Also important, bone and fat have greater resistivity than do blood and muscle. As current flows through the body, it is partitioned among different tissues according to their individual resistivities and volumes. Thus, most of the current used in a body impedance measurement flows through muscle, which has both large volume and low resistivity. Current will also pass through other body components, eg, parenchyma and lymph, but in smaller proportions reflecting their smaller volume fractions in the body. Moreover, muscle is far more conductive in a direction parallel to rather than across the fibers (3), which means that current will preferentially flow along rather than across the direction of muscle fibers.

FREQUENCY DEPENDENCE OF TISSUE PROPERTIES

The resistivity and permittivity of tissues are both strongly dependent on frequency, as discussed at length elsewhere (1). Simple biophysical models can account for this variation (1). The major reason for this frequency dependence, in the frequency range of interest to BIA, is the fact that cellular membranes are poor conductors but good capacitors. Thus, at low frequencies, cells appear electrically as nonconductive objects and current flows primarily through extracellular spaces. At high frequencies, current passes readily through cell membranes because their reactance is low (equation 1), and flows through the intracellular spaces as well.

These ideas can be illustrated by a simple model that applies for a suspension of spherical cells of volume fraction p in a medium of resistivity ρ_a (1). The resistivity at low frequencies ρ_{low} is approximately

$$\rho_{low} \approx \rho_a \frac{(1 + p/2)}{(1 - p)} \approx \frac{3\rho_a}{2} \frac{(1)}{(1 - p)} \quad (11)$$

and, to a good approximation, is inversely proportional to the volume fraction of extracellular fluid $(1 - p)$ if the cell suspension is concentrated. At high frequencies, the current passes through both the intracellular and extracellular fluids and the resistivity of the suspension (for a concentrated suspension) approaches that of the intracellular medium. The transition

frequency, at which the conductivity is halfway between its low- and high-frequency limits, is approximately

$$f_c \approx \frac{1}{\pi r C_m \rho_i} \quad (12)$$

where C_m is the membrane capacitance (in F/m^2), ρ_i is the resistivity of the intracellular medium, and r is the radius of the cell.

For spherical cells in normal physiologic media, this transition frequency is typically in the range of 1–10 MHz. The corresponding transition frequency for the resistivity (ie, the halfway point between its low- and high-frequency limits) occurs at a lower frequency, typically < 0.1 MHz for mathematical reasons (the midpoint in the resistivity is different from the midpoint in the conductivity). For concentrated cell suspensions, the transition frequency for the resistivity corresponds roughly to the frequency at which the current is evenly partitioned between the intracellular and extracellular pathways. In tissues, however, other factors are important (discussed below) and this is not necessarily true in general. This theory for the transition frequency for resistivity can be extended to nonspherical cells and other refinements can also be introduced (1, 4). This simple theory is satisfactory for cell suspensions such as blood and provides a qualitative explanation for the electrical properties of tissues as well (1).

A simple electrical model for a cell suspension or tissue is presented in Figure 3. This shows the extracellular current path that predominates at low frequencies and the intracellular path that is dominant at high frequencies. A plot of the series-equivalent reactance of this circuit (on the vertical axis) versus the series-equivalent resistance (horizontal axis) yields a semi-circular arc (Figure 4). The limiting values of the resistance at low and high frequencies can be found from the intercepts of this arc with the horizontal axis (resistance) as shown in Figure 4.

In this model, the frequency-dependence of the tissue properties arises from the capacitance of the cell membrane, the reactance of which varies as the inverse of the frequency. The electrical behavior of a real tissue is more complex because of its great structural complexity and other effects (1). In tissues the transition between the low-frequency to high-frequency

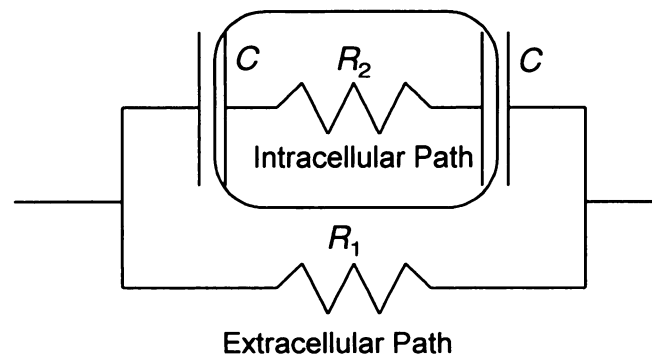


FIGURE 3. Circuit modeling the electrical properties of a cell suspended in physiologic electrolyte. Resistor R_1 models the electrical resistance of the extracellular fluid; resistor R_2 and the capacitors (C) model the impedance to current flowing through the cell (indicated by the broken line). The limiting frequency of this circuit at very low frequencies is $R_1 = R_1$ and at very high frequencies is $R_h = R_1 R_2 / (R_1 + R_2)$.

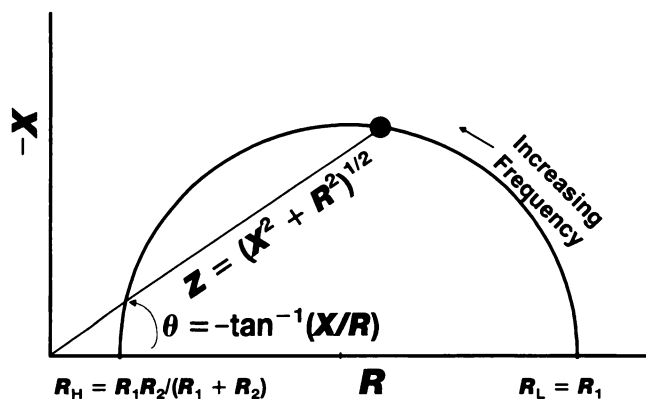


FIGURE 4. Plot of the impedance of the circuit shown in Figure 3 on the complex impedance plane, ie, the real versus the imaginary parts of the circuit impedance. A plot of the reactance X versus the resistance R at different frequencies results in a semicircle. The semicircle intersects the real axis (resistance) at the low- and high-frequency limits R_L and R_H , respectively. The phase angle (θ) and impedance magnitude Z at an arbitrary point are also shown.

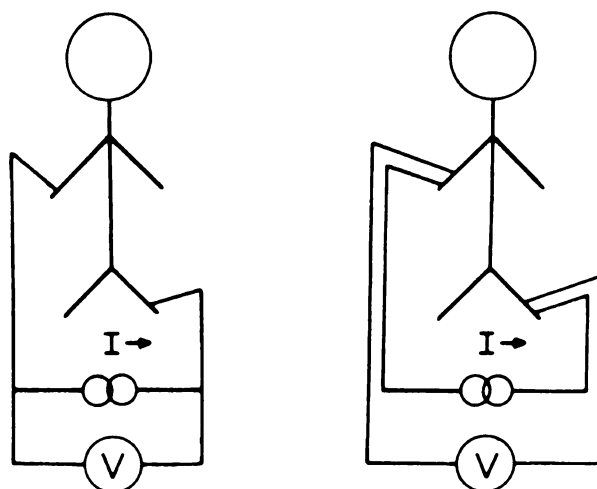
resistivity is a more gradual function of frequency than predicted by the simple model shown in Figure 3. A plot of the resistance versus reactance of tissue characteristically forms a semicircular arc, the center of which is depressed below the real axis (1).

This frequency dependence can be modeled empirically by using a variety of functions, the most widely used of which are Cole-Cole functions [for examples, *see* (1)]. These functions can be fitted to tissue impedance data by using a few adjustable parameters, and make it easier for the investigator to extrapolate tissue impedance data to obtain high- and low-frequency limiting values. They are difficult, however, to interpret in terms of the underlying biophysical mechanisms.

MEASUREMENT OF WHOLE-BODY IMPEDANCE

How impedance of the body is measured is illustrated in **Figure 5**. A small alternating current is passed into the body (often between the wrist and the contralateral ankle) and the corresponding voltage is measured; the impedance is the ratio of voltage to current. For practical reasons of avoiding electrode polarization and minimizing the effects of the impedance of skin beneath the electrodes, investigators use a four-electrode technique, with one pair of electrodes for passing current into the body and another pair for sensing the resulting voltage drop.

BIA makes use of currents (typically 1–10 μA at a frequency of ≥ 10 kHz) that are below the threshold for perception by a factor of one thousand or more (5). We are aware of no published data indicating potential hazards of such small currents. Moreover, the electric fields that are induced in the body are far below the electrical susceptibility limits of devices such as pacemakers or implantable defibrillator-converters, and there is no reason to suspect that an interference problem might exist. In the absence of a detailed safety analysis, however, it would be prudent to avoid performing body impedance measurements on subjects with such devices.



**TWO ELECTRODE
TECHNIQUE**

**FOUR ELECTRODE
TECHNIQUE**

FIGURE 5. Illustration of the measurement of whole-body impedance with a two-electrode or four-electrode technique. The current source passes alternating current of amplitude I through the body and the voltmeter measures the corresponding voltage V that is developed across the body. The complex impedance of the body Z^* is the ratio $V/I \exp(j\theta)$ where θ is the phase-angle difference between the current and the voltage and j is the square root of -1 . Reproduced with permission (6).

SAMPLE IMPEDANCE PLOTS FROM TISSUES AND THE HUMAN BODY

Complex resistivity plots from canine muscle tissue and an impedance plot from a human subject measured from the wrist to the contralateral ankle are shown in **Figure 6** and **Figure 7** (6). In these experiments, the canine tissue was excised from the animals during postmortem examinations (≥ 1 h after death) and placed, with undetermined orientation, in the sample chamber. As expected from the above discussion, both plots (human body impedance and canine muscle impedance) describe semicircular arcs. The transition between the low- and high-frequency limiting values occurs near 50 kHz in both cases. The semicircular arcs with centers below the axis are

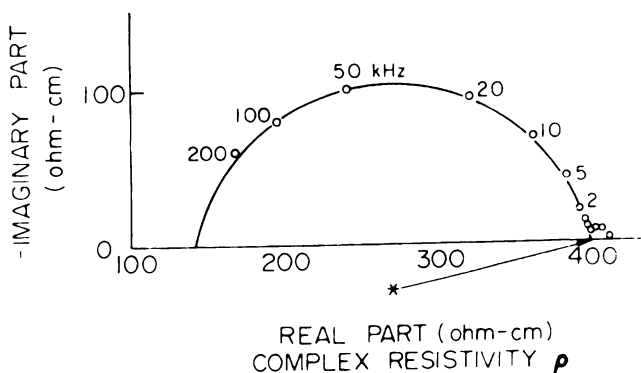


FIGURE 6. Complex impedance properties of canine skeletal muscle, unspecified orientation, at 25 °C. The impedance locus forms a semicircle on the complex plane similar to that predicted for an ideal cell suspension. However, the center of the semicircle is displaced slightly below the real axis, reflecting the heterogeneity of the tissue. Reproduced with permission (6).

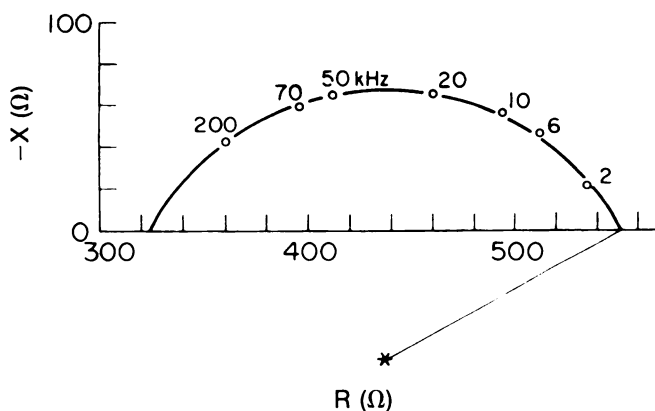


FIGURE 7. Whole-body impedance data from a human subject (from reference 6).

Cole-Cole functions (1), which clearly fit the data well. These figures illustrate how such functions might be used to identify the low- and high-frequency limit values of the resistance, which requires extrapolation outside the frequency range of the reported data.

Both sets of data in Figures 6 and 7 show a similar frequency dependence (ie, a transition or center frequency near 50 kHz). This suggests that the underlying mechanisms are similar both in the excised tissue and in whole-body impedance. Indeed, muscle is the low-resistivity tissue with the greatest volume in the body and will carry the largest fraction of the applied current.

WHAT DOES WHOLE-BODY IMPEDANCE MEASURE?

We now consider the relation between the impedance properties of the body and the clinical indexes that investigators study with BIA, most commonly the volume of a body compartment such as total body water or lean body volume. Empirical relations between body impedance, suitably scaled, and such clinical indexes are well substantiated. For example, the reported SEs in measuring total body water with BIA are typically ≤ 2 L (7). Despite some controversy (8) many investigators report that the technique provides acceptable predictions in cross-sectional studies (6, 9) and longitudinal monitoring of body water in patients (10, 11).

The challenging question is why the method works. Many authors in the BIA literature justify the method with two arguments: 1) a relation exists between the resistance (or impedance) of the body and its volume and 2) at low frequencies, the applied current flows primarily in the extracellular space, whereas at high frequencies the current flows through intracellular space and extracellular volumes as well. Thus, measurements at low frequencies reflect extracellular fluid volumes, whereas those at high frequencies reflect whole-body water. Both of these assumptions can be challenged on obvious biophysical grounds. We discuss each separately.

Relation between impedance and volume

In the example in Figure 2, a simple relation exists between the resistance R and the volume V :

$$V = AL = \frac{\rho L^2}{R} \tag{13}$$

In the body impedance literature, this relation appears repeatedly, with standing height of a subject assumed to represent the conductor length L . This is the basis for scaling body impedance data by the square of the standing height of the subject.

However, equation 13 applies only to cylindrical objects of uniform resistivity. In general, there is no way to determine the volume of an object from its resistance unless its geometry and electrical properties are also known. For example, we consider a body of length L that is rotationally symmetric about its long axis (ie, with a circular cross section; Figure 8). The resistance R between the top and bottom surfaces of the object is given by

$$R = \rho \int_0^L \frac{dz}{\pi r(z)^2} \tag{14}$$

where $r(z)$ is the radius of the structure at height z . The volume V of the object is

$$V = \int_0^L \pi r(z)^2 dz \tag{15}$$

Even in these simple objects, one cannot determine V from R unless the shape [expressed by the function $r(z)$] is known. Figure 8 shows objects with the same resistance between their upper and lower faces, which vary in volume by a factor of nearly 9.

However, objects that are similar in shape (in a geometric sense) and constructed of material with the same resistivity can be compared in volume with impedance measurements. In that case a relation analogous to equation 13 would exist, even though it might not be possible to determine it analytically. Thus, the square of the height of each object divided by its impedance would be perfectly correlated with its volume. This is the fundamental rationale for the use of BIA for determining body volumes. Clearly, if the objects in a collection were all *exactly* similar in a geometric sense, there would be no reason to perform impedance measurements at all. Any index that determines the scale of an object (height, circumference, etc) would be perfectly correlated with its volume. In that case, equation 13 calls for two measurements of scale (impedance and height) but only one measurement is needed.

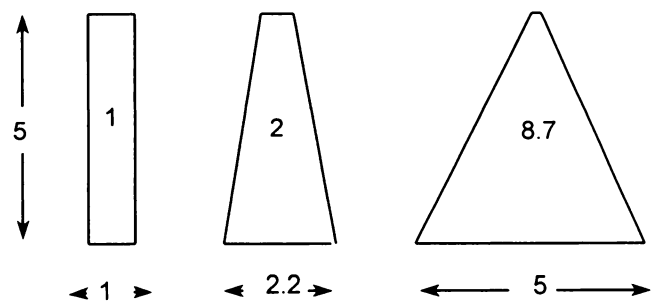


FIGURE 8. Three objects with rotational symmetry about the vertical axis, with the same height but different cross sections. All have the same resistance between the upper and lower surfaces. The height, diameter of the base, and relative volumes of the objects are indicated in the figures.

A situation that is closer to that encountered with BIA is that of a collection of objects that are almost similar in shape. If their shapes are complex, no simple combination of measurements of scale would precisely determine the volume of an individual object. However, simple combinations of such measurements might approximately correlate with the volumes of the objects. To be dimensionally consistent with a volume, the combination of indexes should have dimension (m^3). In that case, impedance measurements might provide information about the scale of an object that could usefully supplement other measurements of scale. Which set of measurements (three of length or two of length plus impedance) correlates best with the volumes of the objects depends on their geometry and the nature of their variability. This empirical issue would be difficult to analyze theoretically.

The geometry of the human body gives rise to another problem with interpretation of the BIA method: most of the measured "whole-body" impedance arises from a small fraction of the total body volume. Several investigators have measured the impedance of defined segments of the body and compared their sum with whole-body impedance. Lukaski and Scheltinga (11) showed that the largest contributors to whole-body resistance are the forearm (28%) and the lower leg (33%), which contribute only 1–2% of the fat-free mass and 1.5–3% of body weight compared with the trunk, which contributes 9% of total resistance and > 50% of fat-free mass and body weight. Other investigators found a discrepancy of $\approx 15\%$ between the sum of the impedance of body segments and the whole-body impedance (12, 13), whereas Lukaski and Scheltinga (11) reported a difference of only 1%. This disparity can be attributed to changing the position of both the source and detecting electrodes, which resulted in the large error compared with that for moving only the detector electrodes. There is no disagreement that the limbs account for most of the whole-body impedance but only a minor fraction of the body volume.

These conclusions are supported by simple numerical calculations. We calculated the impedance of a two-dimensional model of a human assumed to have a uniform resistivity (Figure 9). In this model, a two-dimensional representation of the human body was digitized and electrodes were placed on the wrist and contralateral ankle. The electric field was calculated in the body through use of a finite element program (PDEase; Macsyma Inc, Arlington, MA). The equipotential lines in Figure 9 represent lines of constant voltage. However, the voltage was chosen so that the equipotential lines are numerically equal to the cumulative impedance of the body, measured with respect to the electrode at the ankle. The results of this simple calculation are consistent with the results of Lukaski and Scheltinga (11). Numerical models such as the one shown in Figure 9 can help to explore the sensitivity of the BIA measurements to changes in body geometry and volume and in turn may help clarify the basis of this method. It is clear that small changes in the geometry of distal parts of the leg and arm will result in relatively large changes in body impedance but relatively small changes in body volume. Conversely, changes in the geometry of the torso will hardly affect body impedance but may have a large effect on body volume.

This work leads to an important conclusion: whole-body impedance (as typically measured) is determined primarily by the impedance of the distal parts of the limbs near the electrodes. It is not a strong function of the volume of the body at

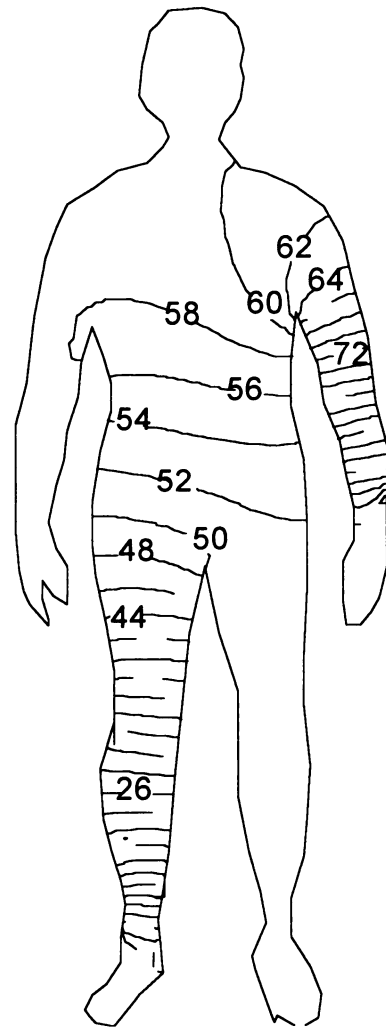


FIGURE 9. Distribution of impedance in the human body. Electrodes were on the wrist and ankle. Numbers indicate the cumulative fraction of impedance (%) relative to the ankle. Each contour is separated by 2% of the total body impedance.

all and its usefulness in body volume measurements is more likely to be as an indirect measure of scale.

Partition of current between intracellular and extracellular spaces

The resistivity of oriented canine skeletal muscle in directions parallel and perpendicular to the fiber axis is shown in Figure 10 (14). The resistivity is nearly 10 times higher in a direction perpendicular, compared with parallel, to the fiber orientation. Moreover, the resistivity is nearly independent of frequency when the current passes parallel to the fibers. This shows that the current passes through the intracellular space in muscle even at low frequencies, when the current is directed along the muscle fibers. Because skeletal muscle fibers are oriented roughly parallel to the long axis of limbs, it follows that current used to measure body impedance will enter the muscle fibers at all frequencies of measurement.

Some investigators have suggested using impedance measurements at low frequencies to estimate extracellular fluid volume, citing equations analogous to equation 11 and making

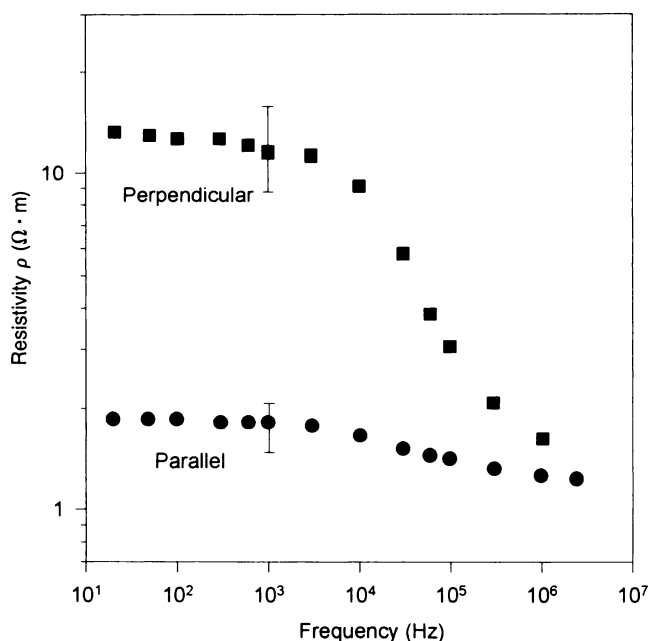


FIGURE 10. Resistivity of canine skeletal muscle oriented in directions parallel and perpendicular to the fiber axis. Error bars represent typical SDs of the data. Redrawn with permission (14).

the assumption that low-frequency current flows primarily through the extracellular space. The extrapolation of this theory (which is well substantiated for suspensions of spherical cells) to muscle tissue is questionable. As the discussion above makes clear, when current flows through muscle tissue in a direction parallel to the fiber direction, it penetrates the intracellular space as well. However, authors have reported useful correlations between low-frequency BIA data from animals and humans and extracellular fluid volumes (15, 16). Perhaps in the wrist and ankle near the electrodes (where most of the body impedance arises) the measurement current flows in a direction largely perpendicular to the direction of muscle fibers and, at least in these regions, remains in the extracellular spaces. The relatively small change in whole-body impedance with frequency (less than a factor of two; compare with Figure 7) suggests that this is not the case, however.

DISCUSSION

The relation between whole-body impedance and body composition is well established experimentally, but, as the above considerations show, is difficult to account for theoretically. Body impedance measurements as usually performed from the wrist to ankle reflect primarily the impedance of limbs in regions near the electrodes and are not strong functions of the whole-body volume at all. To the extent that such measurements reflect global characteristics of the body, the connection is indirect. It is not a causal relation as exists, for example, between the weight of an individual and the reading of a bathroom scale. Nevertheless, substantial and significant relations between impedance variables corrected for stature and indexes of bioconductor volume have been reported by many independent investigators using different reference methods.

This shows the usefulness of impedance measurements for assessing body composition.

Considerable evidence indicates that impedance data can usefully supplement anthropometric measurements. A survey of 250 healthy women and men showed that stature and body weight were significantly correlated with body water, total body potassium, and fat-free mass ($r = 0.73-0.78$, $P < 0.01$) but that resistive impedance was better correlated with these measures of body composition ($r = -0.85$ to -0.90 , $P < 0.001$) (6). When conductor length was approximated with stature and the independent variable $\text{height}^2/\text{resistance}$ was correlated with the various measurements of body composition, strong relations were found ($r = 0.96-0.99$, $P < 0.0001$). Therefore, although simple anthropometric measures such as stature and weight are significant predictors of body composition, the inclusion of impedance data significantly improves the relation with measures of body composition.

This same study showed that the predictive accuracy of using simple anthropometry to estimate body conductor volumes ($\approx 60\%$), estimated by the coefficient of determination, is less than that seen with resistive impedance (81%). The best predictor of estimated bioconductor volume is resistive impedance corrected for stature ($> 92\%$). These and other similar studies provide one level of validation of the working hypothesis that impedance data can be used to infer body composition.

A second level of validation of impedance methods would be to gain an understanding of why the technology works. For this purpose, mathematically derived models and other biophysical analysis can be useful. Three-dimensional models, extending the one shown in Figure 9 and including anatomical information derived from computed tomography, could be developed with data from human volunteers and animals. Such models could be used to explore the interrelated effects of variation of body geometry, body volume, and body impedance. In particular, they might provide a better understanding of the pathways of electrical currents through the body and the relations between body impedance and composition. Computational tools and adequate data exist or could be developed readily for this purpose.

Several areas remain for further development of impedance techniques. Many investigators have compared different measurements of body dimension for use in analyzing impedance measurements. The most common approach is to scale the impedance measurements by the square of the body height. One attempt to standardize for individual differences in body diameter has been to estimate a representative body girth based on measurements of abdominal circumference. Moderate success was achieved when abdominal circumference was used as an independent predictor of body density, an index of body fatness. Thus, additional work is needed to evaluate whether single or multiple measurements of body girth (or other body dimensions) are needed to derive an index of body geometry and scale for use in modeling with impedance measurements.

Another area for further development is the use of impedance methods for the assessment of regional body composition. If regions (eg, upper arm and thigh) of the body with well-defined geometry are measured with impedance devices and reference methods for compositional analysis, a useful application of the technology may be developed for long-term assessment of nutritional status for clinical applications. Fat is poorly conductive and thus is excluded from the current flow.

This suggests that body impedance is more likely to yield clinically useful information about fluid volume and distribution than about body fat.


Other potential improvements in the method have been suggested by investigators or can be anticipated readily. Multifrequency impedance techniques may assist in the determination of fluid volumes when disproportionate changes in the resistivities of intra- and extracellular fluids occur. Also, the utilization of alternative approaches based on established biophysical and engineering models may facilitate estimation of body cell mass and fluid distribution. These include the use of analytical methods that are derived from impedance spectroscopy, eg, the Cole-Cole equations to help identify the low- and high-frequency limits of body resistance, and the novel use of dielectric mixture theory.

Other potential improvements in impedance techniques may involve placement of electrodes at different sites on the body. In particular, electrode placements on the wrist and ankle may be inadequate for assessment of regional accumulation of fluid. This problem has been reported in patients with ascites (17, 18). Some investigators have used other electrode locations to monitor changes in regional fluid depots (19).

As BIA moves out of the research laboratory into general medical practice (and also into use by lay people), further studies will be needed to validate and improve its predictive accuracy. The relation between body impedance and composition is a statistical association, ie, a property of the cohort used to standardize the method. This may lead to potentially large errors when evaluating individuals drawn from a diverse patient population if a clinician uses correlation equations derived from a different group of individuals. Reliability may be a problem when BIA is used under poorly controlled conditions by the lay public. Few studies in the BIA literature have addressed such issues, which are crucial to the use of BIA in general medical practice or outside the clinic.

Impedance methods for determining body composition belong to a large and diverse group of impedance techniques for physiologic measurements, some originating in the early parts of this century (20). Examples include detection of changes in blood volume, accumulation of fluid in the thoracic cavity, and pulsatile blood flow; measurement of cardiac output; and so on. Some of these methods involve impedance measurements over large regions of the body; others (eg, estimation of the flow rate of blood in limbs) involve regional impedance measurements only.

These diverse methods have in common the capability of detecting small changes in electrical properties of the body, a consequence of the high precision that is possible with impedance measurements. Their limitations typically are related to the difficulty in interpreting impedance data quantitatively, given the anatomical and electrical complexity of the body and the impossibility of controlling precisely where the current flows in the body. Similar strengths and limitations are evident in the use of bioelectrical impedance in body-composition analysis as well. In conclusion, the use of impedance techniques for assessment of human body composition is a rapidly evolving area of research. As biologists and engineers collaborate in developing new models and validation studies of BIA,

future advancements of the technology for in vivo assessment of body composition will become manifest. 

REFERENCES

1. Foster KR, Schwan HP. Dielectric properties of tissues—a critical review. *CRC Crit Rev Bioeng* 1989;17:25–104.
2. Löfgren B. The electrical impedance of a complex tissue and its relation to changes in volume and fluid distribution; study on rat kidneys. *Acta Physiol Scand* 1951;23(suppl 81):1–51.
3. Epstein BR, Foster KR. Anisotropy in the dielectric properties of skeletal muscle. *Med Biol Eng Comp* 1983;21:51–5.
4. Hanai T. Electrical properties of emulsions. In: Sherman PH, ed. *Emulsion science*. London: Academic Press, 1968:354–477.
5. Dalziel CF. The threshold of perception of currents. *IEEE Trans Power Apparatus Systems* 1954;73:990–6.
6. Settle RG, Foster KR, Epstein BR, Mullen JL. Nutritional assessment: whole-body impedance and body fluid compartments. *Nutr Cancer* 1980;2:72–80.
7. Lukaski HC. Applications of bioelectrical impedance analysis: a critical review. In: Yasumura S, Harrison JE, McNeill KG, Woodhead AD, Dilmanian FA, eds. *In vivo body composition studies*. New York: Plenum Press, 1990:365–74.
8. Cohn SH. How valid are bioelectric impedance measurements in body composition studies? *Am J Clin Nutr* 1985;42:889–90.
9. Kushner RF, Schoeller DA, Fjeld KR, Danford L. Is the impedance index (ht^2/R) significant in predicting total body water? *Am J Clin Nutr* 1992;56:835–9.
10. Meguid MM, Lukaski HC, Tripp MD, Rosenburg JM, Parker FB. Rapid bedside method to assess change in postoperative fluid status using bioelectrical impedance analysis. *Surgery* 1992;112:502–8.
11. Lukaski HC, Scheltinga MAR. Improved sensitivity of the tetrapolar bioelectrical impedance technique to assess fluid status and body composition: use of proximal electrode placement. *Age Nutr* 1994;5:123–9.
12. Baumgartner RN, Chumlea WC, Roche AF. Estimation of body composition from bioelectric impedance of body segments. *Am J Clin Nutr* 1989;50:221–6.
13. Fuller NJ, Elia M. Potential use of bioelectrical impedance of the whole body and of body segments for the assessment of body composition: comparison with densitometry and anthropometry. *Eur J Clin Nutr* 1989;43:779–91.
14. Epstein BR, Foster KR. Anisotropy in the dielectric properties of skeletal muscle. *Med Biol Eng Comp* 1983;21:51–5.
15. Cornish BH, Ward LC, Thomas BJ. Measurement of extracellular and total body water of rats using multiple frequency bioelectrical impedance analysis. *Nutr Res* 1992;12:657–66.
16. Van Loan MD, Kopp LE, King JC, Wong WW, Mayclin PL. Fluid changes during pregnancy—use of bioimpedance spectroscopy. *J Appl Physiol* 1995;78:1037–42.
17. Gugliemi FW, Contento F, Laddaga L, Panella C, Francavilla A. Bioelectrical impedance analysis: experience with male patients with cirrhosis. *Hepatology* 1991;13:892–5.
18. Zillikens MC, van den Berg JWO, Wilson JHP, Swart GR. Whole-body and segmental bioelectrical-impedance analysis in patients with cirrhosis of the liver: changes after treatment of ascites. *Am J Clin Nutr* 1992;55:621–5.
19. DeVries PMJM, Kouw PM, Olthof CG, et al. A segmental multifrequency conductivity technique to measure dynamic body fluid changes. *Age Nutr* 1994;5:118–22.
20. Geddes LA, Baker LE. *Principles of applied biomedical instrumentation*. 3rd ed. New York: Wiley-Interscience, 1989.